Journal Pre-proof

Study on the kinetics and energy transfer during ignition of methane excited by NRP-SDBD non-equilibrium plasma

Ziying Xin, Zhencao Zheng, Yong Hu, Ruijiao Cao, Ao Sun, Feiyang Zhao, Wenbin Yu

PII: S1743-9671(24)00407-0

DOI: https://doi.org/10.1016/j.joei.2024.101929

Reference: JOEI 101929

To appear in: *Journal of the Energy Institute*

Received Date: 25 August 2024

Revised Date: 29 November 2024

Accepted Date: 6 December 2024

Please cite this article as: Z. Xin, Z. Zheng, Y. Hu, R. Cao, A. Sun, F. Zhao, W. Yu, Study on the kinetics and energy transfer during ignition of methane excited by NRP-SDBD non-equilibrium plasma, *Journal of the Energy Institute*, https://doi.org/10.1016/j.joei.2024.101929.

Study on the kinetics and energy transfer during ignition of methane excited by NRP-SDBD non-equilibrium plasma

Ziying Xin[a], Zhencao Zheng[a], Yong Hu[a], Ruijiao Cao[a], Ao Sun[a], Feiyang Zhao[a,b]*Wenbin Yu[a,b*]

a. School of energy and power engineering, Shandong University, Jinan, Shandong, 250061, China

b. Shenzhen Research Institute of Shandong University, Shenzhen, Guangdong, 518057, China

** Corresponding author: Email address: fyzhao@sdu.edu.cn (Dr. FY Zhao), wbyu@sdu.edu.cn(Dr. WB Yu)*

Abstract

The energy deposition distribution is crucial factor during plasma assisted ignition (PAI) influenced by streamer morphology, electric field, electron density and gas temperature. This paper presents numerical studies on energy transfer induced by gas heating and kinetic enhancement effect during ignition of lean and stoichiometric $CH_4/O_2/He$ mixture excited by NRP-SDBD plasma. The two-dimensional plasma solver PASSKEy is employed to analyse hydrodynamic perturbation in a very small time-spatial scale for $CH_4/O_2/He$ mixture with different equivalence ratios. A faster early perturbation response after plasma excitation occurs for stoichiometric $CH_4/O_2/He$ mixture owing to more concentrated energy release. The plasma-participant path flux analysis model is newly developed to reveal the kinetic effects of key plasma species, dominant global reaction paths for oxidation of CH_4. It is highlighted that the important role of CH_4(v13) and O(1D) enriched at higher PRF by plasma-oriented kinetic reactions on formation of active radical O atoms and key intermediate CH_3. High PRF is beneficial for release of H atoms along with the reduced consumption for O_2 on the global reaction path of conversion from CH_4 to CO_2. Ultimately, the energy efficiency of gas heating is discussed from the view of plasma kinetics. The enrichment of O(1D) and charged species owing to improved PRF facilitates increase in the proportion of total discharge energy spent on gas heating attributed to the quenching reactions of O(1D) and recombination reactions of charged particles.

Keywords: Plasma assisted ignition; Combustion kinetics; Energy transfer; Global reaction path; Gas heating

1 Introduction

The lean combustion of natural gas has remarkable advantages in improving engine thermal efficiency while reducing pollutant emissions. However, the ultra-lean mixture combustion is still facing main challenges in significant cycle-to-cycle variability or even misfires. The non-equilibrium plasma gives unprecedented opportunity for combustion enhancement and emission mitigation, due to its great potential in altering conventional S-curve[1], promoting ignition[2,3], extending flammability limits[4], improving flame stability[5], accelerating low-temperature fuel oxidation[6], and fuel reforming[7,8].

The nanosecond repetitive pulsed surface dielectric barrier discharge (NRP-SDBD) is a promising method to generate large-area and uniform non-equilibrium plasma with more kinetic activity and higher energy density. Non-equilibrium plasma assisted combustion/ ignition (PAC/PAI) at atmospheric pressure and low initial temperature can be accomplished via various enhancement pathways including thermal effect, kinetic effect and transport effect[9-11]. The electrons run away from the atoms and transform into highly energetic free electrons under the influence of applied electric field. Subsequently, the energy transfer from the high-energy electrons into surrounding gas molecules occurs by inelastic collision. The rising of temperature due to the increase in internal energy of gas molecules facilitates acceleration of chemical reactions as well as fuel oxidation according to the Arrhenius equation, knows as the thermal effect. Moreover, the activated particles taken as “chemical combustion promoters” and strong oxidizing free radicals are generated by electron impact reactions between high-energy electrons and reactant molecules (i.e. vibrational and electronic excitation, ionization, and dissociation), resulting in reduced activation barriers and accelerated chain reactions, which refers to kinetic effect. Meanwhile, the transport effect responses to the ion wind effect associated with the enhanced mixing of reactants.

The positive PAC/PAI process is basically determined by the energy deposition influenced by the gas temperature, the electric field, ionization degree, and discharge morphology[12]. Many researches have reported the results of quantitative studies involving numerical or experimental in-situ diagnosis investigations into the effects of combustion enhancement as well as gas heating during PAC/PAI processes. The experimental techniques for diagnosis of key parameters mainly include spectroscopy measurements for electric field[13], schlieren or shadow imaging related to energy release[14], optical emission spectroscopy (OES)[15,16] and picosecond CARS spectroscopy[17] to measure gas temperature. Zhao Q et al.[18] developed the transient high-frequency nanosecond surface dielectric barrier discharge (nSDBD) system for ignition of stoichiometric propane/air mixtures at ambient initial temperature and pressure in constant volume combustion chamber. The spatial distribution characteristics of discharge filaments through multi-channel nSDBD were revealed, to assess the promoting effects on initiation of flame kernel. Furthermore, the minimum ignition energy used to ignite propane/air mixtures with stable flame propagation speeds was therefore reported. The influence of gas pressure and discharge energy on flame propagation of lean propane/air mixtures ignited by high voltage NRP discharge on pin-to-pin electrode was investigated by Xu et al.[19]. The study examined the superiority with higher flame propagation speed motivated by NRP discharge compared to conventional spark ignition. In numerical simulation, the zero-dimensional program that couples plasma kinetics solver ZDPlasKin and chemical reaction kinetics solver CHEMKIN was widely applied to model the interplay between non-equilibrium plasma processes and hydrocarbon oxidation. The reduced electric field (E/N, where E is the electric field and N is the gas number density) was usually set as a constant value during repetitive nanosecond pulse stage used as hybrid ZDPlasKin-CHEMKIN model input to study ignition enhancement effects of

non-equilibrium plasma on ignition of reactants[20-23]. A modified model based on SENKIN and ZDPlaskin code has been developed by Qiu Y et al.[24] to investigate ignition delay and emission characteristics of NO for combustion of $NH_3/N_2/O_2$ mixtures excited by hybrid repetitive nanosecond and DC discharge plasma. It was found that O(1D) promoted ignition via NH_3+O(1D)→NH_2+OH through sensitivity analysis, and NH_3(v2) played the dominated role in heat release via V-T relaxation reaction NH_3(v2)+NH_3→2NH_3.

Gas heating is also one of significant factors affecting discharge energy deposition during PAC/PAI process. The local temperature rise owing to fast gas heating (FGH)[25] resulting from quenching of electronic excitation species within tens-hundreds of nanoseconds and slow gas heating[26] caused by V-T relaxation on microsecond timescales can (i) accelerate chemical reactions; (ii) create hydrodynamic perturbation due to the propagation of pressure waves. The ignition in the whole combustion chamber is facilitated by the propagation of combustion waves. It was demonstrated that the propagation of combustion waves can be accelerated owing to the interaction between hydrodynamic perturbation and combustion waves if gas heating within the ignition regions occurs on a shorter timescale than typical gas-dynamic time[27-30]. The gas heating effects combined with the generation of active species play an important role in reducing ignition delay and improving flame stability of lean combustion. Moreover, the gas heating is able to induce plasma thermal instability[31,32] so that trigger positive feedback of discharge enhancement processes. The plasma thermal instability refers to closed-loop including positive feedback of gas temperature, gas density, reduced electric field, electron density, Joule heat, etc. ($T\uparrow \rightarrow N\downarrow \rightarrow E/N\uparrow \rightarrow ne\uparrow \rightarrow jE\uparrow \rightarrow T\uparrow$). The combustion kinetics reactions can either decelerate or accelerate the occurrence of instability known as thermal-chemical instability[33-35]. The plasma destabilization will lead to redistribution of deposited energy and

transition of discharge mode from homogeneous state to contracted state, thus disturb phase-transition from streamer to spark during NRP discharges. The kinetic models, energy efficiency and characteristic time of gas heating were closely monitored in previous studies. The proportion of total energy deposition attributed to fast gas heating during nanosecond pulsed discharge on pin-to-pin electrode was calculated by Xu et al.[36]. It was showed that most of discharge energy could be rapidly converted into gas heating within tens of nanoseconds, approximately 75% of the discharge energy can be effectively transformed into gas heating when E/N is increased to 270Td and initial gas temperature is 2000±500 K. The compression waves generated in nitrogen and air mixtures at P=100Torr during nanosecond pulsed discharge on spherical electrode were observed by Montello et al.[37]. It was concluded that the characteristic time of rapid temperature rise in air was approximately 100ns, which was considerably shorter than in nitrogen (1μs). The numerical simulation of gas heating under nanosecond pulsed discharge in H_2/air mixtures at an initial temperature of 1000K and atmospheric pressure was carried out by Kobayashi et al.[38]. It was found that the generation of O(3P), H and OH, as well as temperature increase were mainly attributed to quenching of $N_2(A^3\sum_u^+)$, $N_2(B^3\Pi_g)$, $N_2(C^3\Pi_u)$ by O(1D) and H_2, along with quenching of O(1D) by H_2. White et al.[39] measured the characteristic time of V-T relaxation reactions related to O_2(v) and C_xH_y at T=430-1350K for stoichiometric C_2H_4/O_2 mixtures. It was observed that V-T relaxation occured in a shorter time scale than typical gas-dynamic time for ambient pressure above 1bar, while the heat release due to V-T relaxation affected the formation and propagation of combustion waves.

As mentioned above, the microscopic parameters such as E/N and electron density are the most important for controlling ignition enhancement and flame stabilization during PAC/PAI process, but these parameters are difficult to measure in real-time and situ through

the experiments. Furthermore, hydrodynamic perturbation and plasma thermal instability caused by gas heating will influence the distributions of deposited energy, those should be taken most care to be addressed. In the light of the issue above, the objective of this study is to explore the nonlinear synergetic interaction between streamer propagation of NRP-SDBD plasma, energy transfer induced by gas heating and plasma kinetics during non-equilibrium PAI on $CH_4/O_2/He$ mixtures. Firstly, the hydrodynamic perturbations initiated by fast gas heating in $CH_4/O_2/He$ mixtures with different equivalence ratios are compared, in order to qualitatively analyze the early response of the fluid after plasma excitation in a very short time and small spatial scale. Secondly, the dominant global reaction paths connecting source species to sink species are disclosed in the perspective of both plasma and chemical kinetics using time-evolution of electric field during streamer propagation as inputs of hybrid ZDPlasKin-CHEMKIN model. Meanwhile, the normalized sensitivity coefficient for ignition delay time are systematically analyzed to qualify the importance of key reactions. Finally, the energy efficiency of gas heating attributed to plasma-oriented kinetic reactions during PAI of $CH_4/O_2/He$ mixtures is evaluated.

2 Hydrodynamic perturbation initiated by nSDBD in $CH_4/O_2/He$ mixtures

In our previous study[40], a simplified plasma kinetics mechanism of $CH_4/O_2/He$ mixtures has been developed based on P-DRGEP (Plasma-targeted Directed Relation Graph with Error Propagation) algorithm and path flux analysis, to mitigate the computational loads of modeling nSDBD by the two-dimensional plasma solver PASSKEy[41]. The mechanism was well calibrated by reaction gas temperature and energy branching. A two-dimensional streamer propagation model initiated by nSDBD plasma in $CH_4/O_2/He$ mixtures was set up, which showed good performance in predicting the characteristics of discharge current on peak value, changing trend and phase. Moreover, as the ionization wave propagates forward,

the sequential and spatial distributions of electric field were extracted, which would be used as inputs in following plasma-chemical kinetic modeling.

In aspect of plasma kinetics, the inelastic collisions between high-energy electrons and gas molecules occur under the excitation of nSDBD, accompanying with energy transfer. The rates of heat release caused by relaxation and quenching of excited species as well as recombination of charged particles are much greater than those by outward diffusion, hence leading to localized high-temperature and pressure waves. It was found[42-45] that the propagation speed of pressure waves was at supersonic speed in the initial discharge stage and subsequently decayed to the level of sound speed within the time range of microsecond to millisecond due to thermal diffusion and air resistance. Nevertheless, it is difficult to measure hydrodynamic perturbation on nanosecond time scale by experimental methods.

In this section, as the Electron Energy Distribution Function (EEDF) changes with mixture composition, the pressure perturbation on nanosecond to sub-microsecond time scale due to local gas heating induced by nSDBD is modeled by PASSKEy for both stoichiometric and lean (ϕ=0.5) CH_4/O_2 mixtures with 75% helium dilution. The discharge voltage is set to triangular waves of 15kV in amplitude and 50ns on the rising as well as falling edges. The schematic diagram of electrode shape and computational domain with mesh layout is given in Figure 1. The space-time distributions of gas pressure from the end of discharge to the early afterglow stage (t<1us) in $CH_4/O_2/He$ medium at ϕ=1 and ϕ=0.5 are depicted in Figure 2 and Figure 3, respectively. It can be observed that pressure wave is initiated at the interface between the bare electrode and the upper surface of dielectric, and propagates outward along the direction perpendicular to the surface of dielectric.

In order to quantify hydrodynamic perturbation under different gas mixture media, the propagation speed within the nanosecond to sub-microsecond time scale is formulated by

fitting the propagation distance of the pressure wave against time as shown in Figure 4. The calculated propagation speed of the pressure wave is 606.95m/s when $\phi=1$, whereas for $\phi=0.5$, it is recorded as 577.50m/s. Additionally, it is found that the total heat release for $\phi=1$ is 1.1652 times greater than that with $\phi=0.5$ based on calculated the total fast gas heating energy deposition of each reactions. From this standpoint, it is speculated that there is more concentrated energy release and higher heating rate for surrounding gas when $\phi=1$, which facilitates stronger perturbation and faster propagation speed of pressure waves.

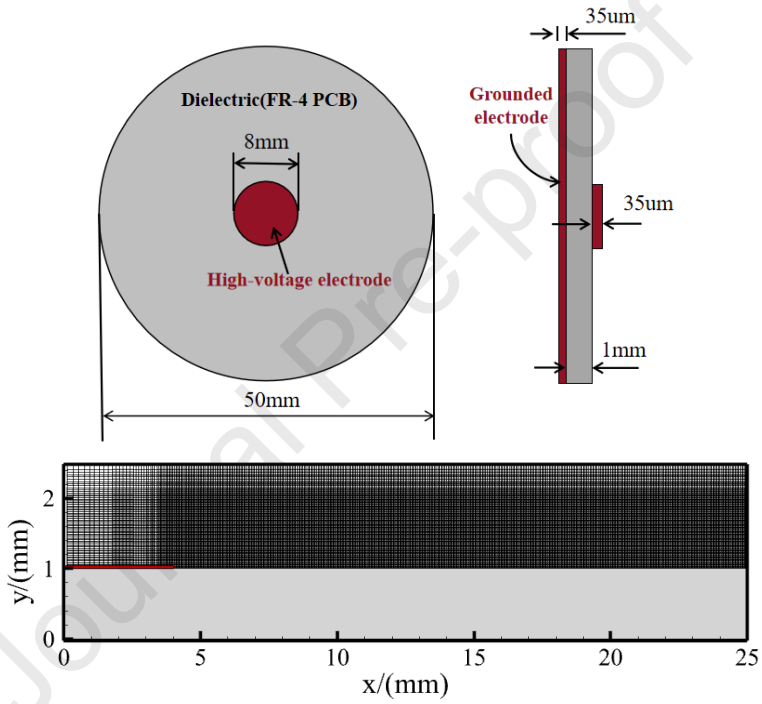

Fig.1. The schematic diagram of electrode shape, computational domain and mesh distribution

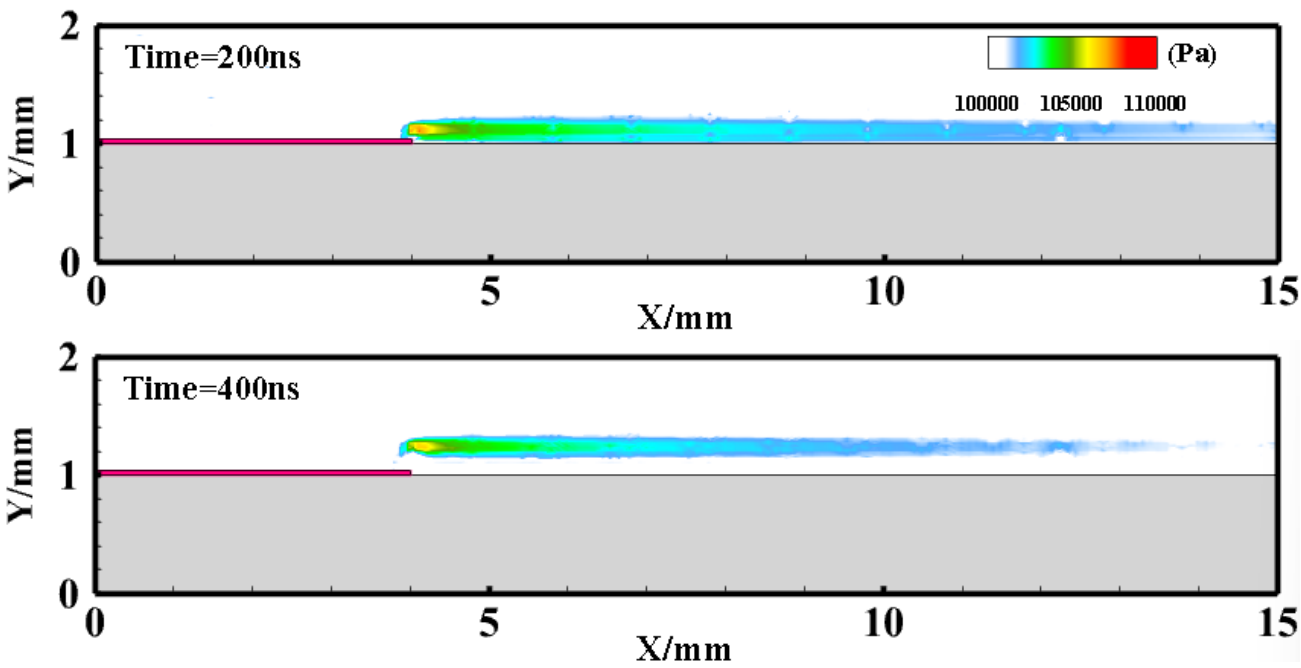

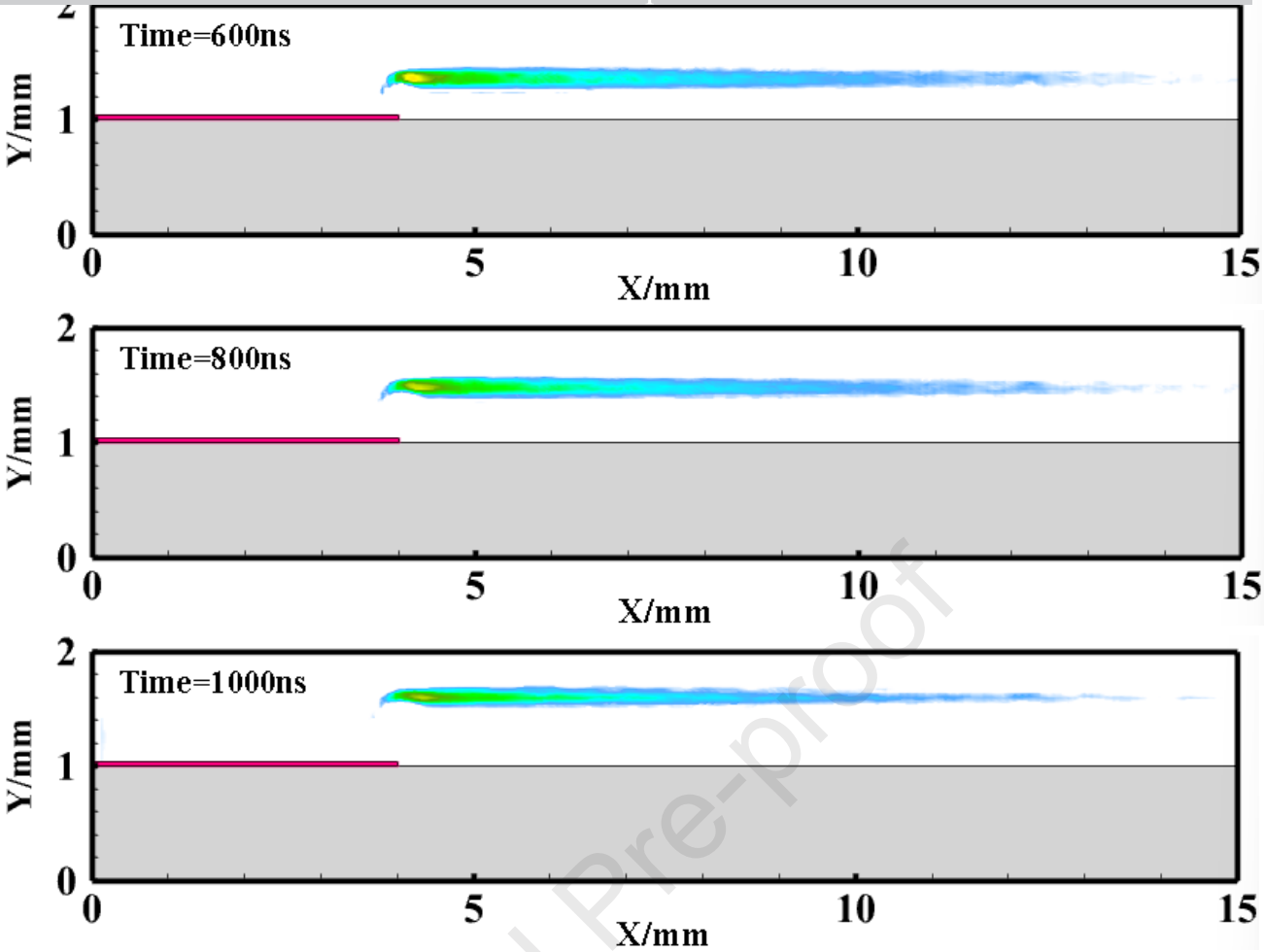

Fig.2. The evolution of the calculated pressure perturbations (in Pa) under nSDBD excitation for $0.083CH_4/0.167O_2/0.75He$ plasma

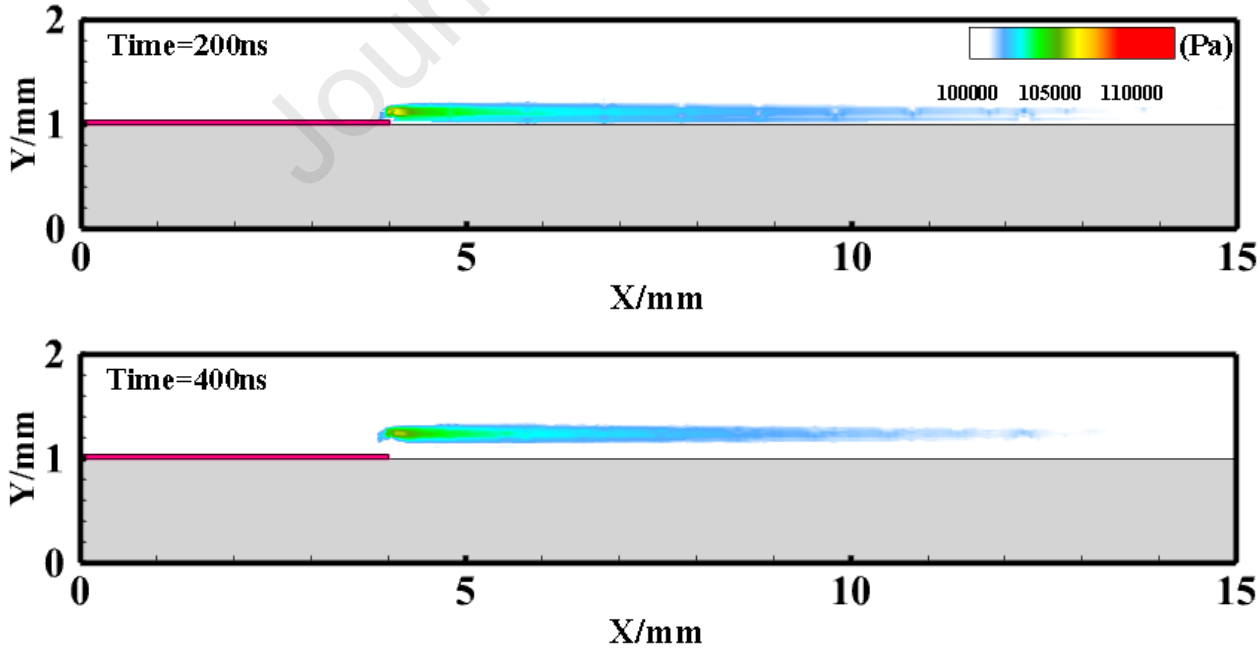

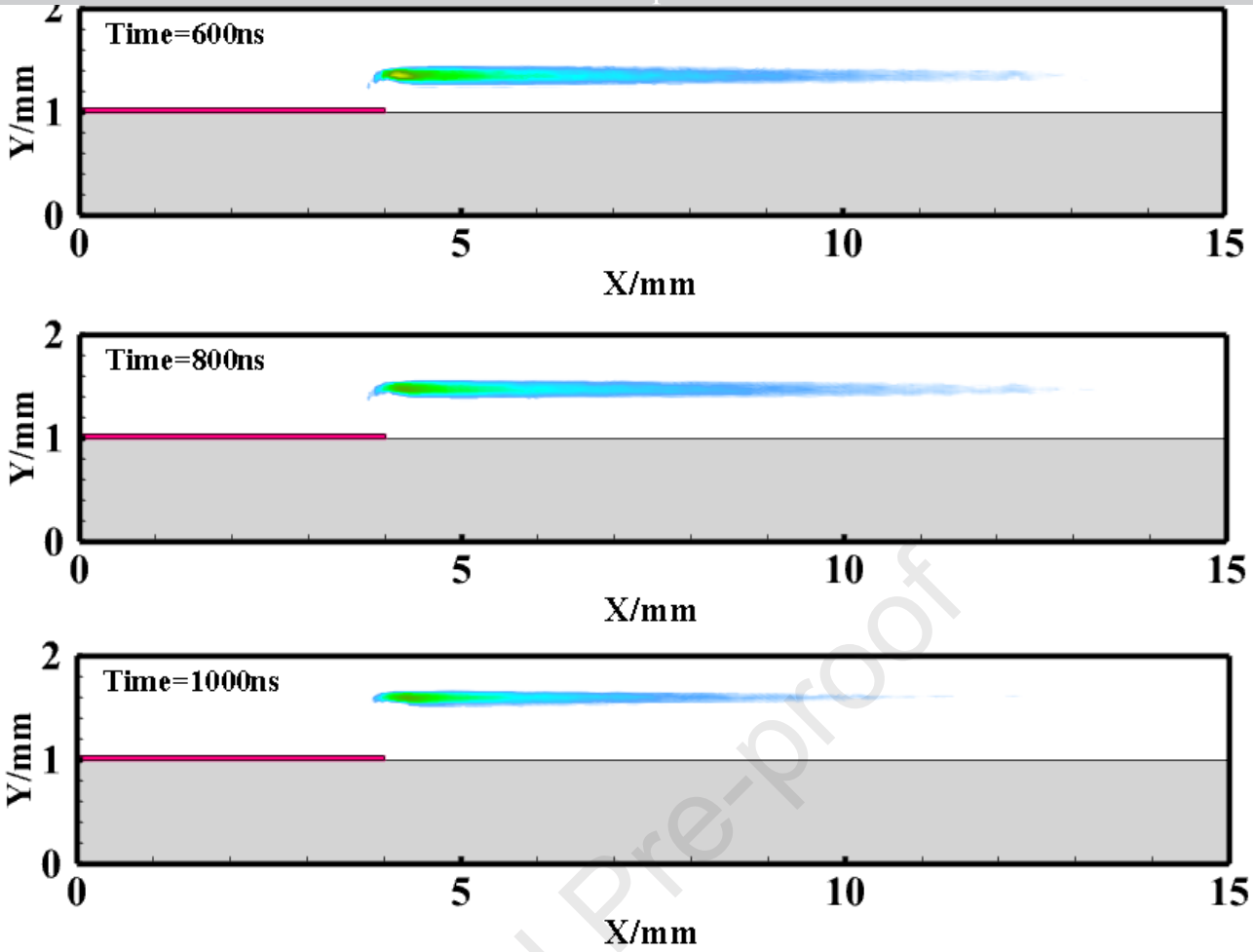

Fig.3. The evolution of the calculated pressure perturbations (in Pa) under nSDBD excitation for $0.05CH_4/0.20O_2/0.75He$ plasma

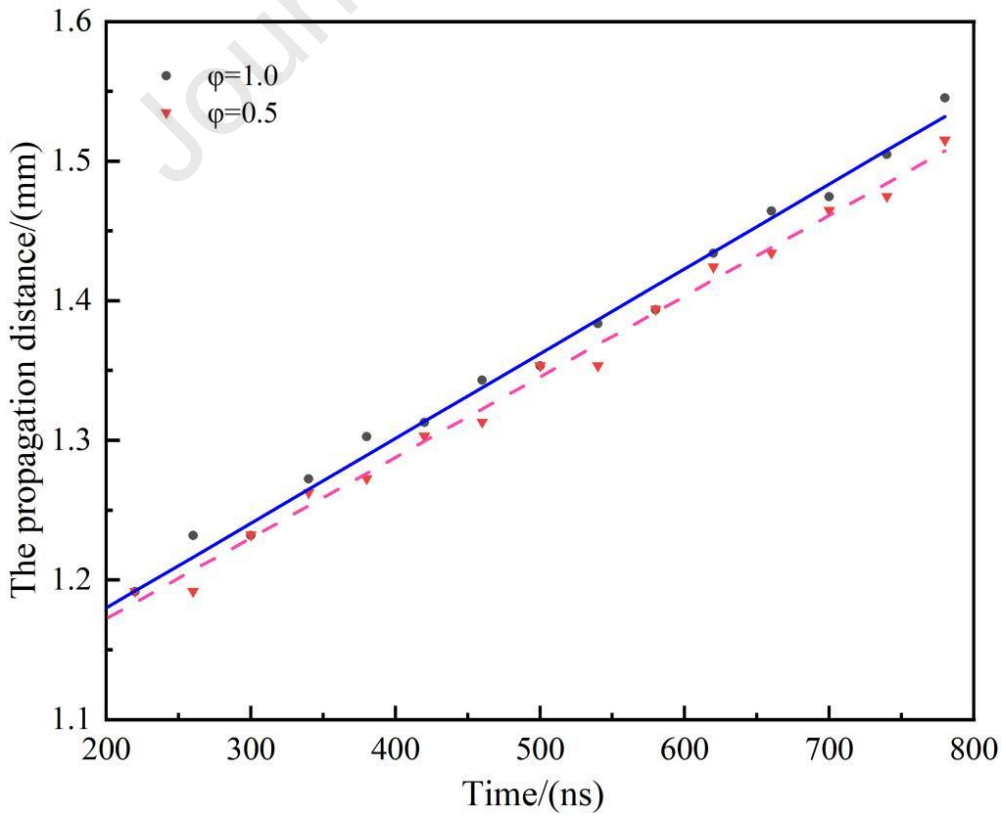

Fig.4. The propagation distance of pressure wave induced by nSDBD for stoichiometric and lean CH_4/O_2 mixtures with 75% helium dilution

3 Simulation of ignition of $CH_4/O_2/He$ mixtures excited by NRP-SDBD plasma

In this study, a zero-dimensional model incorporating the plasma kinetics solver ZDPlasKin and the combustion chemical kinetics solver CHEMKIN is used to explore the effects of pulse repetition frequency (PRF) on low temperature ignition of lean and stoichiometric $CH_4/O_2/He$ mixtures excited by NRP-SDBD plasma, in which the electric field against time curve E(t) during streamer propagation extracted at probed point near the center of the two-dimensional discharge field (x=14.5, y=1.1mm) calculated by PASSKEy is dynamically interpolated as shown in Figure 5. The initial electron density is set to 10^8 cm^{-3} estimated based on the given power density.

The time evolution of electron density, E/N and gas temperature during PAI for stoichiometric and lean (ϕ=0.5) CH_4/O_2 mixtures with 75% helium dilution at different PRF (20kHz/100kHz) is displayed in Figure 6. It can be observed that ignition occurs after three discharge pulses for ϕ=1.0 at PRF=20kHz, while gas temperature has no significant change after few pulses for ϕ=0.5 at the same PRF, which is mainly owing to less energy deposition and weakened kinetic effect. The details explanation is available in our previous study[40] considering the length of this paper. Compared with ϕ=0.5 at PRF=20kHz, increasing the PRF to 100kHz enables the lean $CH_4/O_2/He$ mixture to be ignited successfully after several pulses.

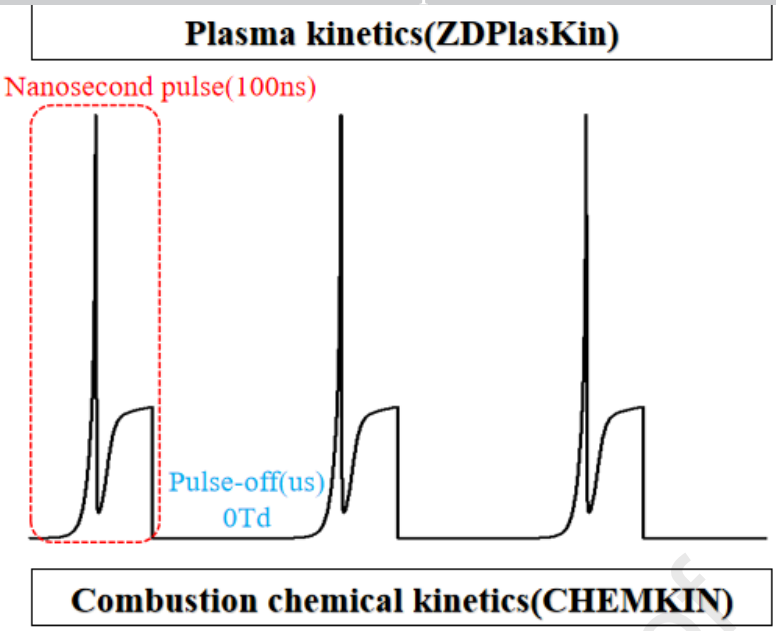

Fig.5. Schematic diagram of electric field excitation

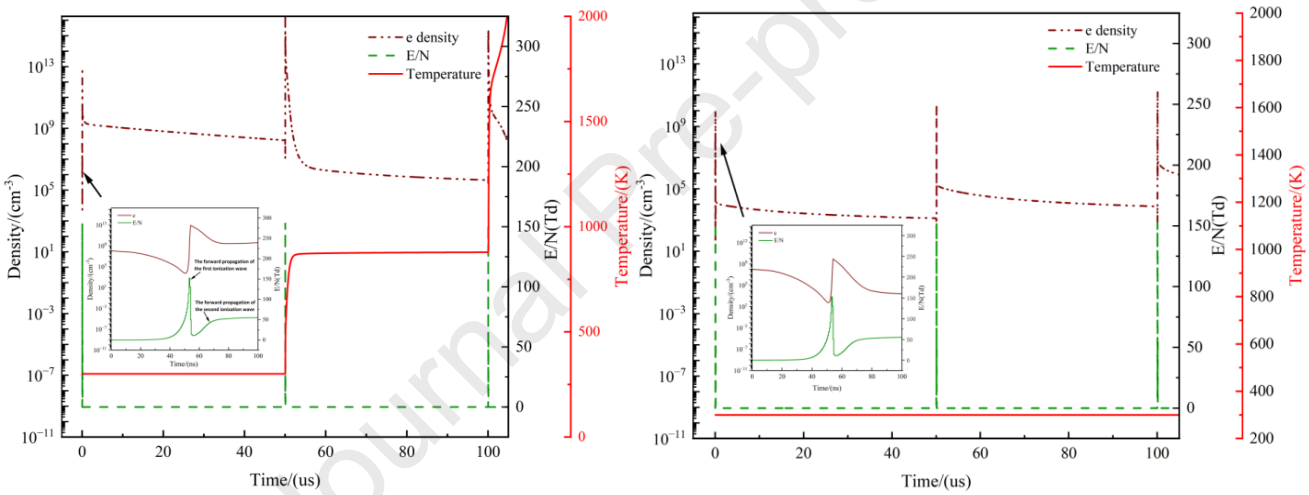

(a) Φ=1,PRF=20kHz **(b) Φ=0.5,PRF=20kHz**

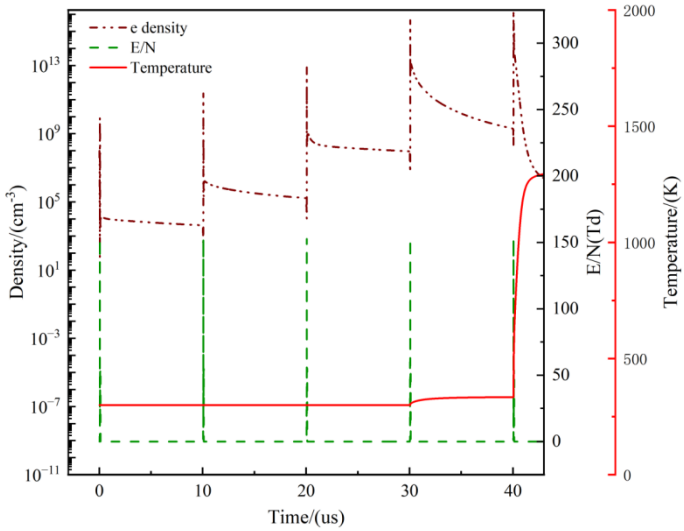

(c) Φ=0.5,PRF=100kHz

Fig.6. Time evolution of electron density, E/N and gas temperature for stoichiometric and lean (Φ=0.5) CH_4/O_2/He mixtures excited by NRP-SDBD at different PRF

3.1 Kinetic effects motivated by NRP-SDBD plasma on ignition of $CH_4/O_2/He$ mixtures

3.1.1 Global path flux analysis

The stoichiometric coefficient matrix and reaction rate matrix are calculated to evaluate the contribution rate of each reaction to the generation of species dominated in PAI. The reaction path diagrams are elaborately depicted for $CH_4/O_2/He$ mixtures at $\phi=1$ with PRF=20kHz and $\phi=0.5$ with PRF=100kHz as shown in Figure 7 and Figure 8, respectively. The non-equilibrium excitation of NRP-SDBD plasma promotes the production of active species such as O atoms, singlet oxygen atoms O(1D) and singlet oxygen molecule $O_2(a^1\Delta_g)$, which directly accelerate the generation of CH_2OH and CH_3O, as well as indirectly facilitate the formation of important ignition intermediates CH_3, CH_2O and HCO via kinetic effect. It is observed that O(1D) mainly comes from electron impact dissociation reaction via $E+O_2\rightarrow E+O+O(1D)$, while most of $O_2(a^1\Delta_g)$ are produced from electronic excitation reaction via $E+O_2\rightarrow E + O_2(a^1\Delta_g)$. It is worthwhile to note that O atoms mainly comes from chemical reaction via $H+O_2\rightarrow O+OH$ for $\phi=1.0$ with PRF=20kHz. Nevertheless, for $\phi=0.5$ with PRF=100kHz, most of O atoms are derived from plasma reactions including electron impact dissociation $E+O_2\rightarrow E+O+O/O(1D)$, quenching of $O_2(b^1\Sigma_g^+)$ via $O_2(b^1\Sigma_g^+)+H\rightarrow OH+O$, and quenching of O(1D) via $O(1D)+O_2\rightarrow O+O_2(b^1\Sigma_g^+)$. Moreover, CH_3 is outstanding towards the formation of C_2H_y and CH_2O. While for $\phi=1.0$ with PRF=20kHz, CH_3 primarily comes from the chemical reactions between CH_4 and active radicals OH/H/O. It is noteworthy that two active species participant paths are the major sources of CH_3 formation at $\phi=0.5$ with PRF=100kHz, via $CH_4(v13)+O\rightarrow CH_3+OH$ and $O(1D)+CH_4\rightarrow CH_3+OH$, respectively. Consequently, it can be inferred that improving the PRF enriches the activated species like O(1D) and $CH_4(v13)$, thereby the PAI process is enhanced with plasma kinetic effects.

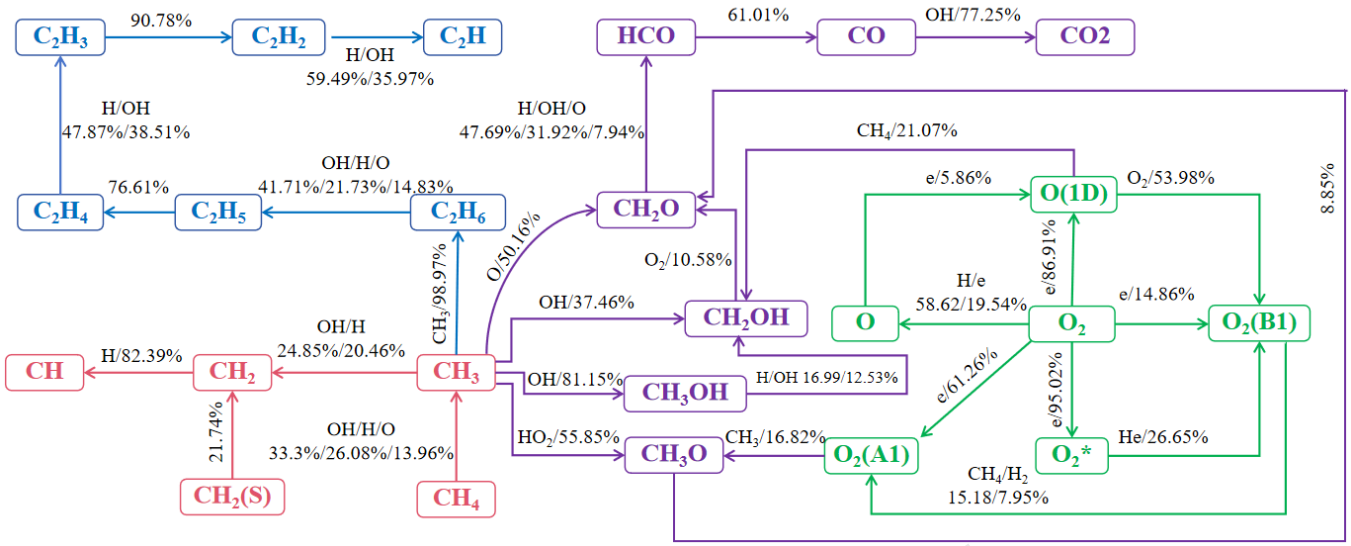

Fig.7. The reaction path diagram for Φ=1 and PRF=20kHz

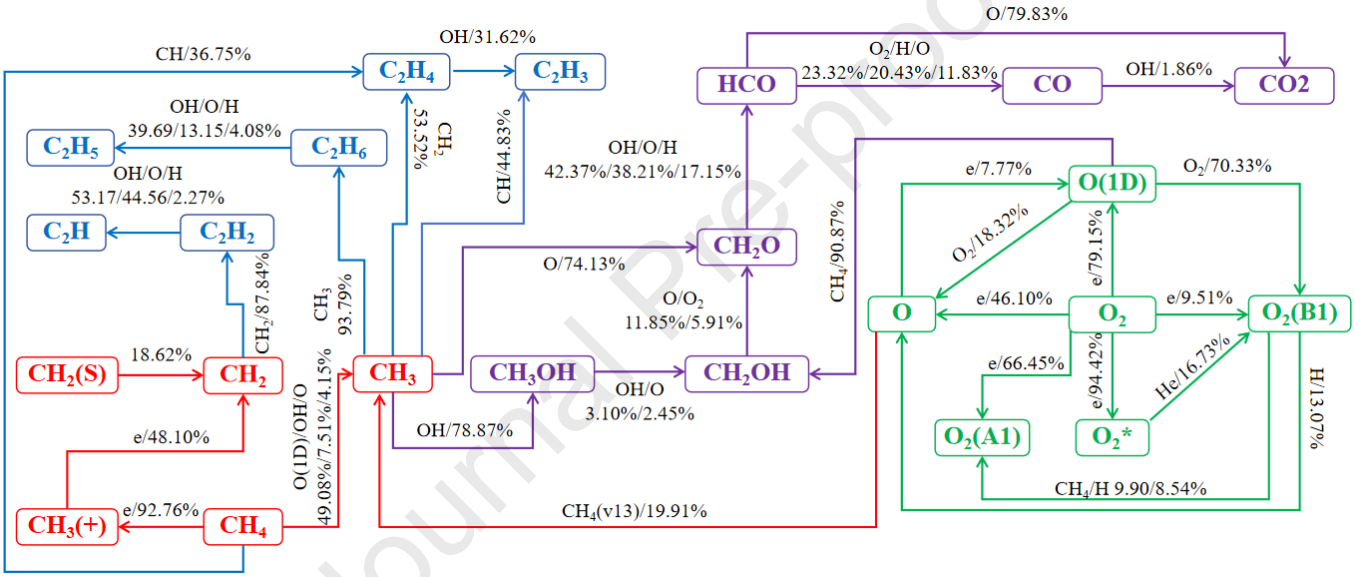

Fig.8. The reaction path diagram for Φ=0.5 and PRF=100kHz

To further assess the kinetics of PAI systems, the global pathways analysis (GPA)[46] and Depth First Search (DFS) algorithm[47] are employed to uncover transformation from the initial reactants to the final products. It features with identifying dominant global reaction paths ($S_0 \rightarrow \cdots S_i \rightarrow \cdots \rightarrow S_j$) connecting source species to sink species through important hub species based on constructed element flux graphs in plasma-assisted systems. Firstly, the element flux transfer going from the *i-th* species to the *j-th* species $A_{e,i\rightarrow j}$ is calculated by

$$A_{e,i\rightarrow j} = \sum_r a_{e,r,i\rightarrow j} \tag{1}$$

where $a_{e,r,i\rightarrow j}$ is the element flux transfer of the *e-th* element going from the *i-th* species to

the *j-th* species through the *r-th* reaction. Meanwhile, $a_{e,r,i\to j}$ is given by

$$a_{e,r,i\to j} = \max(0, C_{e,r,i\to j} w_r) \tag{2}$$

where w_r is the rate of the *r-th* reaction. The positive element flux $C_{e,r,i\to j}$ from the *i-th* species to the *j-th* species is obtained by

$$C_{e,r,i\to j} = \begin{cases} n_{e,r,j} \dfrac{n_{e,r,i}}{n_{e,r}}, v_{r,j} v_{r,i} < 0 \\ 0, otherwise \end{cases} \tag{3}$$

where $n_{e,r,i}$ represents the number of the *e-th* element going out from the *i-th* species in the *r-th* reaction, and $n_{e,r,j}$ represents the number of the *e-th* element going into the *j-th* species in the *r-th* reaction. $n_{e,r}$ represents the number of the *e-th* element in the *r-th* reaction. Subsequently, the DFS algorithm is used to pinpoint all global pathways from source species to sink species based on element flux transfer matrix. In this study, the parameter $D_{GP,e}$ is defined to figure out the dominant global pathways governing the element flux of source species given by formula (4). The calculation flowchart of global path analysis is shown in Figure 9.

$$D_{GP,e} = D_{source,e} D_{GP/source,e} \tag{4}$$

Where $D_{source,e}$ is the ratio of total number of the *e-th* atom in the source species to the total number of the initial *e-th* atom. $D_{GP/source,e}$ represents geometric mean of the fractions of the *e-th* atoms distributed to the conversion steps of global pathway, in which n_{GP} represents the number of conversion steps in the global pathway.

$$D_{GP/source,e} = \left(\prod_{i,j\in GP} \frac{A_{e,i\to j}}{\sum_k a_{e,i\to k}} \right)^{\frac{1}{n_{GP}}} \tag{5}$$

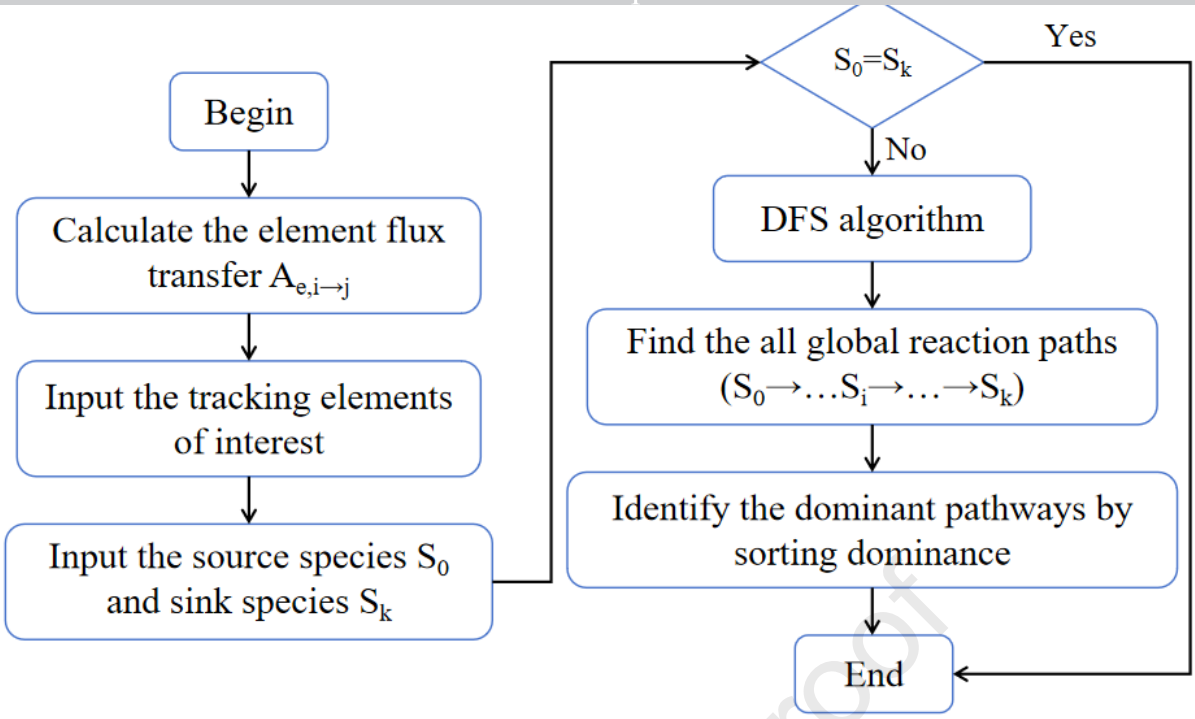

Fig.9. The calculation flowchart of global path flux analysis

The source species CH_4 and sink species CO_2 are selected as characteristic particles to monitor the migration of the element C. The dominant global reaction paths for conversion from CH_4 to CO_2 are screened and sorted based on parameter $D_{GP,e}$ as shown in Table 1 and Table 2, respectively. When $\phi=1$ and PRF=20kHz, the dominant global reaction pathway for oxidation of CH_4 is as follows: CH_4=>CH_3=>CH_2O=>HCO=>CO=>CO_2. The intermediate oxide CO is mainly originated from HCO via HCO+O_2=>CO+HO_2 and HCO +H=>CO+H_2. While for $\phi=0.5$ and PRF=100kHz, the primary pathway for conversion from CH_4 to CO_2 is CH_4=>CH_3=>CH_2O=>HCO=>CO_2. The species HCO is directly transformed into CO_2 through the reaction HCO+O=>CO_2+H, resulting in the release of H atoms as well as reduced consumption of O_2 and H atoms.

Table 1 The global reaction pathway chains for conversion from CH_4 to CO_2 for $\phi=1$ and PRF=20kHz

The global reaction pathway chains	$D_{GP,e}$
CH_4=>CH_3=>CH_2O=>HCO=>CO=>CO_2	2.5972e-02
CH_4=>CH_4(V13)=>CH_3=>CH_2O =>HCO=>CO=>CO_2	1.5903e-02
CH_4=>CH_3=>CO=>CO_2	1.5067e-02
CH_4=>CH_3=>CH_2OH =>CH_2O=>HCO=>CO=>CO_2	1.4620e-02
CH_4=>CH_4(V24)=>CH_3=>CH_2O=>HCO=>CO=>CO_2	1.4542e-02

Table 2 The global reaction pathway chains for conversion from CH_4 to CO_2 for Φ=0.5 and PRF=100kHz

The global reaction pathway chains	$D_{GP,e}$
CH_4=>CH_3=>CH_2O=>HCO=>CO_2	4.9700e-02
CH_4 =>CH_3=>CH_2O=>HCO=>CO=>CO_2	4.1971e-02
CH_4=>CH_4(V13)=>CH_3=>CH_2O=>HCO=>CO_2	3.8024e-02
CH_4=>CH_4(V13)=>CH_3=>CH_2O=>HCO=>CO=>CO_2	3.4536e-02
CH_4=>CH_4(V24)=>CH_3=>CH_2O=> HCO =>CO_2	3.3094e-02

3.1.2 Sensitivity analysis

In this section, the sensitivity analysis is carried out to explore the influence of plasma kinetic reactions on ignition delay time. The normalized sensitivity coefficient of ignition delay *S* is defined by formula (6). A negative sensitivity coefficient indicates that the plasma reaction promotes ignition enhancement.

$$S = \frac{\tau(2rrt(i)) - \tau(rrt(i))}{\tau(rrt(i))} \tag{6}$$

Where τ is the ignition delay time, $rrt(i)$ is the rate constant of the *i-th* reaction.

Figure 10 displays the normalized sensitivity coefficients of plasma involved kinetic reactions which have significant influence on ignition delay time during NRP-SDBD plasma assisted combustion of stoichiometric and lean (ϕ=0.5) $CH_4/O_2/He$ mixtures. It can be observed that ionization reactions E+O_2=>E+E+O_2^+, E+CH_4=>E+E+CH_4^+, E+CH_4=>E+E+CH_3^++H, and E+He=>E+E+He^+ have the most pronounced effects on ignition enhancement, indicating a positive correlation between production of electron and reduction of ignition delay time. The positive sensitivity coefficients of electron attachment reactions via E+O_2=>O_2^- and E+O_2=>O+O^- further validate this conclusion. The normalized sensitivity coefficient of E+O_2=>E+O+O(1D) is -0.4973 for ϕ=1 and PRF=20kHz, which is -0.2663 when ϕ=0.5 and PRF=100kHz. The finding suggests that the production of O and singlet O(1D) originated from dissociation reaction of O_2 facilitates ignition enhancement. Furthermore, the sensitivity coefficients of recombination reactions of charged species via O_2^-+O_2^+=>O_2+O_2 and O^-+O^+=>O+O for ϕ=0.5 and PRF=100kHz are -0.2214

and -0.2206, respectively. It can be concluded that recombination reactions promote ignition at high PRF attributed to enriched charged species.

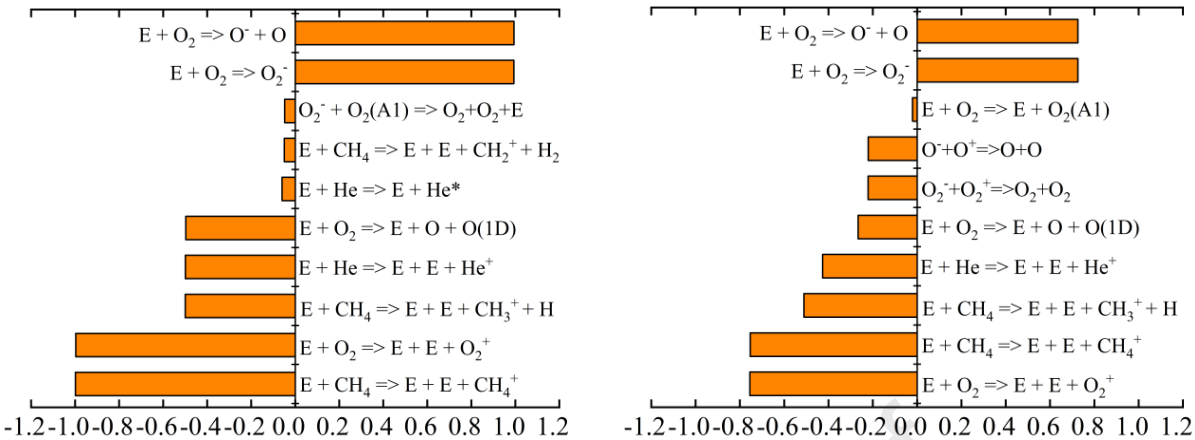

(a) Φ =1, PRF=20kHz **(b) Φ =0.5, PRF=100kHz**

Fig.10. The normalized sensitivity coefficients of plasma kinetic reactions for ignition delay time

3.2 Gas heating induced energy transfer during PAI for $CH_4/O_2/He$ mixtures

From the view of plasma kinetics, the relaxation of vibrationally excited species, quenching of electronically excited species, as well as recombination of charged particles will contribute to discharge energy transfer due to gas heating. In this section, the proportion of heat deposition during PAI for $CH_4/O_2/He$ mixtures is calculated for Φ =1.0 with PRF=20kHz and Φ =0.5 with PRF=100kHz, as tabulated in Table 3 and Table 4, respectively. Wherein, the heat release can be calculated using formula (7), where Δh_r represents the reaction enthalpy and q_r is the rate of the r-th reaction. The energy efficiency n_R is defined to quantify the proportion of total discharge energy spent on gas heating.

$$Q_r = q_r \Delta h_r \tag{7}$$

The energy efficiency of gas heating attributed to the quenching of O(1D) by CH_4, O_2 and CH_2O is taken 9.7461% and 13.3649% for Φ =1.0 with PRF=20kHz and Φ =0.5 with PRF=100kHz, respectively. Figure 11 displays the density of O(1D) against time curve during PAI for stoichiometric and lean (Φ =0.5) $CH_4/O_2/He$ mixtures at different PRF

(20kHz/100kHz). It can be observed that ignition in lean mixture (ϕ=0.5) at the lower PRF (20kHz) is not conducive to the production of O(1D). The efficiency in generating O(1D) is the highest for ϕ=0.5 and PRF=100kHz, indicating that the enrichment of O (1D) should be attributed to shortened pulse interval. Moreover, the total energy efficiency of gas heating owing to electron-ion recombination and ion-ion recombination is 3.8207% and 9.9649% for ϕ=1.0 with PRF=20kHz and ϕ=0.5 with PRF=100kHz, respectively. This indicates that more O(1D) and charged species such as electrons and CH_3^+ are generated by increasing PRF, as well as more concentrated energy is deposited. In addition, the quenching reactions of O_2* and O_2(B1) are also the main sources initiating gas heating. The deposited heating caused by relaxation reactions of CH_4(v13) accounts for 1.3510% of the total discharge energy when ϕ=1 and PRF=20kHz, nevertheless such deposited heating is quite small for ϕ=0.5 and PRF=100kHz due to the characteristic time of relaxation of CH_4(v13) exceeding the pulse interval for PRF=100kHz.

Overall, the global path flux analysis and sensitivity analysis for ignition of lean and stoichiometric $CH_4/O_2/He$ mixtures motivated by NRP-SDBD plasma at different PRF are compared, meanwhile the energy transfer efficiency induced by gas heating is discussed, providing valuable insights into assess the kinetics of plasma-assisted systems and energy relaxation in discharges in hydrocarbon-based mixtures.

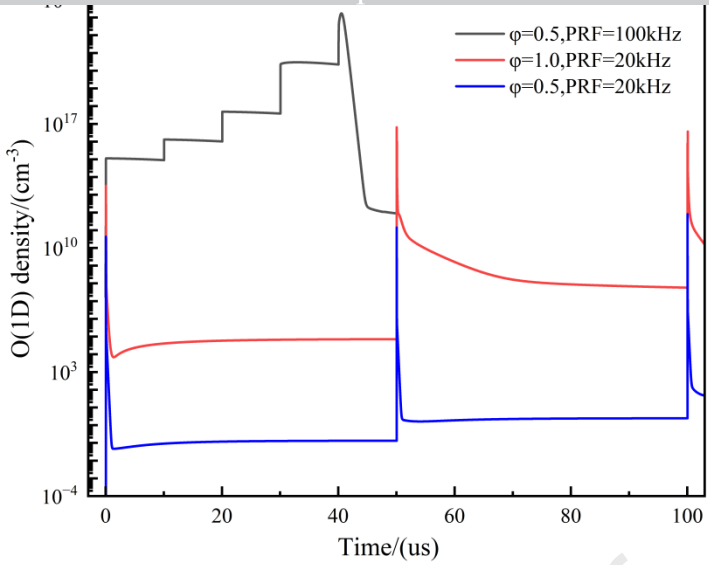

Fig.11. The density of O(1D) vs time during PAI of stoichiometric and lean (Φ =0.5) $CH_4/O_2/He$ mixtures under different PRF(20kHz and 100kHz)

Table 3 The main sources of gas heating for Φ = 1 and PRF=20kHz

Reaction class	η_R (%)
The quenching reactions of O(1D) by $CH_4/O_2/CH_2O$	9.7461
The recombination reactions of electron and CH_3^+/O_2^+	1.9826
The recombination reactions of O_2^- and O_2^+	1.8381
The quenching reactions of O_2* by He	1.4589
The relaxation reactions of CH_4(v13)	1.3510
The quenching reactions of O_2(B1) by H	0.7766

Table 4 The main sources of gas heating for Φ = 0.5 and PRF=100kHz

Reaction class	η_R (%)
The quenching reactions of O(1D) by $CH_4/O_2/CH_2O$	13.3649
The recombination reactions of electron and $CH_3^+/CH_4^+/O_2^+/O^+$	6.9921
The recombination reactions of O^-/O_2^- and O_2^+	2.9728
The quenching reactions of O_2* by He	1.7010

4 Conclusions

The discharge energy transfer triggered by gas heating during ignition of stoichiometric and lean $CH_4/O_2/He$ mixtures excited by NRP-SDBD plasma are numerically studied. Meanwhile, the path flux analysis model is constructed to explore the kinetic enhancement effects of dominated species in plasma-assisted systems and global reaction paths connecting source species to sink species. Main conclusions can be drawn from this work, as follows:

(1)The propagation characteristic of pressure waves after nSDBD excitation is simulated by two-dimensional plasma solver PASSKEy. The hydrodynamic perturbations caused by fast gas heating in stoichiometric and lean (ϕ=0.5) $CH_4/O_2/He$ mixtures within the nanosecond to sub-microsecond time scale are compared. The calculated propagation speed of pressure wave is higher in stoichiometric $CH_4/O_2/He$ mixtures, which is owing to more concentrated energy released.

(2)The path flux analysis model in plasma-participant system is developed to quantify impact weight of dominated species on ignition enhancement. It was found that active species such as O, O(1D), O_2(A1) generated under the excitation of NRP-SDBD plasma accelerate the production of important ignition intermediates CH_3, CH_2O and HCO. It is noteworthy that for the case of ϕ=1 and PRF=20kHz, O atoms and CH_3 mainly come from chemical reactions, while for the case of ϕ=0.5 and PRF=100kHz, most of O atoms are derived from electron impact dissociation and quenching reactions of excited species, CH_3 mainly originates from plasma reactions involving CH_4(v13) and O(1D). The release of H atoms along with the reduced consumption for O_2 are achieved by increasing PRF on the global reaction pathway of methane oxidation.

(3)The energy efficiency of gas heating during PAI of stoichiometric and lean(ϕ=0.5) $CH_4/O_2/He$ mixtures at different PRF is calculated. The more concentrated energy is deposited at higher PRF, leading to enrichment of O(1D) and charged species, thereby promoting increase in the proportion of total discharge energy spent on gas heating owing to the quenching reactions of O(1D) and recombination reactions of charged particles. The energy efficiency of gas heating due to relaxation of CH_4(v13) is higher for ϕ=0.5 with PRF=100kHz compared to ϕ=1.0 with PRF=20kHz, which is attributed to the characteristic time of relaxation of CH_4(v13) exceeding the pulse interval when PRF=100kHz.

Acknowledgement

The authors greatly acknowledge the support of National Natural Science Foundation of China (No. 52406145) and Shandong Provincial Natural Science Foundation(No. ZR2022QE268 and No. 2022HWYQ-061) and Guangdong Basic and Applied Basic Research Foundation (No. 2022A1515110571)

References

[1] Won S H, Jiang B, Diévart P, et al. Self-sustaining n-heptane cool diffusion flames activated by ozone[J]. Proceedings of the Combustion Institute, 2015, 35(1): 881-888.

[2] Popov N A. Kinetics of plasma-assisted combustion: effect of non-equilibrium excitation on the ignition and oxidation of combustible mixtures[J]. Plasma Sources Science and Technology, 2016, 25(4): 043002.

[3] Starikovskiy A, Aleksandrov N, Rakitin A. Plasma-assisted ignition and deflagration-to-detonation transition[J]. Philosophical Transactions of the Royal Society A: Mathematical, Physical and Engineering Sciences, 2012, 370(1960): 740-773.

[4] Zhao H, Zhao N, Zhang T, et al. Studies of multi-channel spark ignition of lean n-pentane/air mixtures in a spherical chamber[J]. Combustion and Flame, 2020, 212: 337-344.

[5] Sun J, Tang Y, Li S. Plasma-assisted stabilization of premixed swirl flames by gliding arc discharges[J]. Proceedings of the Combustion Institute, 2021, 38(4): 6733-6741.

[6] Zhang R, Liao H, Yang J, et al. Exploring chemical kinetics of plasma assisted oxidation of dimethyl ether (DME)[J]. Combustion and Flame, 2021, 225: 388-394.

[7] Sun J, Chen Q, Guo Y, et al. Quantitative behavior of vibrational excitation in AC plasma assisted dry reforming of methane[J]. Journal of Energy Chemistry, 2020, 46: 133-143.

[8] Mao X, Chen Q, Guo C. Methane pyrolysis with N2/Ar/He diluents in a repetitively-pulsed nanosecond discharge: Kinetics development for plasma assisted combustion and fuel reforming[J]. Energy Conversion and Management, 2019, 200: 112018.

[9] Ju Y, Sun W. Plasma assisted combustion: Progress, challenges, and opportunities[J]. Combustion and Flame, 2015, 162(3): 529-532.

[10] Ju Y, Sun W. Plasma assisted combustion: Dynamics and chemistry[J]. Progress in Energy and Combustion Science, 2015, 48: 21-83.

[11] Ju Y, Lefkowitz J K, Reuter C B, et al. Plasma assisted low temperature combustion[J]. Plasma Chemistry and Plasma Processing, 2016, 36: 85-105.

[12] DeFilippo A C, Chen J Y. Modeling plasma-assisted methane–air ignition using pre-calculated electron impact reaction rates[J]. Combustion and Flame, 2016, 172: 38-48.

[13] Stepanyan S A, Soloviev V R, Starikovskaia S M. An electric field in nanosecond surface dielectric barrier discharge at different polarities of the high voltage pulse: spectroscopy measurements and numerical modeling[J]. Journal of Physics D: Applied Physics, 2014, 47(48): 485201.

[14] Xu D A, Shneider M N, Lacoste D A, et al. Thermal and hydrodynamic effects of nanosecond discharges in atmospheric pressure air[J]. Journal of Physics D: Applied Physics, 2014, 47(23): 235202.

[15] Aleksandrov N L, Kindysheva S V, Nudnova M M, et al. Mechanism of ultra-fast heating in a non-equilibrium weakly ionized air discharge plasma in high electric fields[J]. Journal of Physics D: Applied Physics, 2010, 43(25): 255201.

[16] Lo A, Cessou A, Boubert P, et al. Space and time analysis of the nanosecond scale discharges in atmospheric pressure air: I. Gas temperature and vibrational distribution function of N2 and O2[J]. Journal of Physics D: Applied Physics, 2014, 47(11): 115201.

[17] Montello A, Burnette D, Nishihara M, et al. Dynamics of rapid localized heating in nanosecond pulse discharges for high speed flow control[J]. Journal of Fluid Science and Technology, 2013, 8(2): 147-159.

[18] Zhao Q, Xiong Y, Yang X, et al. Experimental study on multi-channel ignition of propane-air by transient repetitive nanosecond surface dielectric barrier discharge[J]. Fuel, 2022, 324: 124723.

[19] Xu D A, Lacoste D A, Laux C O. Ignition of quiescent lean propane–air mixtures at high pressure by nanosecond repetitively pulsed discharges[J]. Plasma Chemistry and Plasma Processing, 2016, 36: 309-327.

[20] Mao X, Chen Q, Rousso A C, et al. Effects of controlled non-equilibrium excitation on H2/O2/He ignition using a hybrid repetitive nanosecond and DC discharge[J]. Combustion and Flame, 2019, 206: 522-535.

[21] Mao X, Rousso A, Chen Q, et al. Numerical modeling of ignition enhancement of CH4/O2/He mixtures using a hybrid repetitive nanosecond and DC discharge[J]. Proceedings of the Combustion Institute, 2019, 37(4): 5545-5552.

[22] Faingold G, Lefkowitz J K. A numerical investigation of NH3/O2/He ignition limits in a non-thermal plasma[J]. Proceedings of the Combustion Institute, 2021, 38(4): 6661-6669.

[23] Ban Y, Zhang F, Zhong S, et al. The numerical simulation of nanosecond-pulsed discharge-assisted ignition in lean-burn natural gas HCCI engines[J]. Frontiers in Mechanical Engineering, 2022, 8: 930109.

[24] Qiu Y, Zhu Y, Wu Y, et al. Numerical investigation of the hybrid pulse–DC plasma assisted ignition and

NOx emission of NH3/N2/O2 mixture[J]. Combustion and Flame, 2023, 258: 113078.

[25] Popov N A, Starikovskaia S M. Relaxation of electronic excitation in nitrogen/oxygen and fuel/air mixtures: fast gas heating in plasma-assisted ignition and flame stabilization[J]. Progress in Energy and Combustion Science, 2022, 91: 100928.

[26] Gordiets B F, Osipov A I, Stupochenko E V, et al. Vibrational relaxation in gases and molecular lasers[J]. Soviet Physics Uspekhi, 1973, 15(6): 759.

[27] Liberman MA. Introduction to physics and chemistry of combustion. Explosion, flame, detonation. Berlin, Heidelberg: Springer-V; 2008.

[28] Berezhetskaya N K, Gritsinin S I, Kop'ev V A, et al. Ignition of a combustible gas mixture by a high-current electric discharge in a closed volume[J]. Plasma physics reports, 2009, 35: 471-483.

[29] Maley L, Bhattacharjee R, Lau-Chapdelaine S M, et al. Influence of hydrodynamic instabilities on the propagation mechanism of fast flames[J]. Proceedings of the Combustion Institute, 2015, 35(2): 2117-2126.

[30] Shcherbanev S A, Popov N A, Starikovskaia S M. Ignition of high pressure lean H2: air mixtures along the multiple channels of nanosecond surface discharge[J]. Combustion and Flame, 2017, 176: 272-284.

[31] Golubovskii Y B, Nekuchaev V, Gorchakov S, et al. Contraction of the positive column of discharges in noble gases[J]. Plasma Sources Science and Technology, 2011, 20(5): 053002.

[32] Shneider M N, Mokrov M S, Milikh G M. Dynamic contraction of the positive column of a self-sustained glow discharge in air flow[J]. Physics of Plasmas, 2014, 21(3).

[33] Rousso A C, Goldberg B M, Chen T Y, et al. Time and space resolved diagnostics for plasma thermal-chemical instability of fuel oxidation in nanosecond plasma discharges[J]. Plasma Sources Science and Technology, 2020, 29(10): 105012.

[34] Zhong H, Shneider M N, Mokrov M S, et al. Thermal-chemical instability of weakly ionized plasma in a reactive flow[J]. Journal of Physics D: Applied Physics, 2019, 52(48): 484001.

[35] Zhong H, Shneider M N, Mao X, et al. Dynamics and chemical mode analysis of plasma thermal-chemical instability[J]. Plasma Sources Science and Technology, 2021, 30(3): 035002.

[36] Xu D A, Shneider M N, Lacoste D A, et al. Thermal and hydrodynamic effects of nanosecond discharges in atmospheric pressure air[J]. Journal of Physics D: Applied Physics, 2014, 47(23): 235202.

[37] Montello A, Burnette D, Nishihara M, et al. Dynamics of rapid localized heating in nanosecond pulse discharges for high speed flow control[J]. Journal of Fluid Science and Technology, 2013, 8(2): 147-159.

[38] Kobayashi S, Bonaventura Z, Tholin F, et al. Study of nanosecond discharges in H2–air mixtures at atmospheric pressure for plasma assisted combustion applications[J]. Plasma Sources Science and

Technology, 2017, 26(7): 075004.

[39] White D R. Vibrational relaxation of oxygen by methane, acetylene, and ethylene[J]. The Journal of Chemical Physics, 1965, 42(6): 2028-2032.

[40] Xin Z, Zheng Z, Hu Y, et al. Numerical modeling of plasma assisted ignition of CH4/O2/He mixture by the nanosecond repetitive pulsed surface dielectric barrier discharge[J]. Fuel, 2024, 357: 129975.

[41] Zhu Y, Shcherbanev S, Baron B, et al. Nanosecond surface dielectric barrier discharge in atmospheric pressure air: I. measurements and 2D modeling of morphology, propagation and hydrodynamic perturbations[J]. Plasma Sources Science and Technology, 2017, 26(12): 125004.

[42] Bayoda K D, Benard N, Moreau E. Elongating the area of plasma/fluid interaction of surface nanosecond pulsed discharges[J]. Journal of Electrostatics, 2015, 74: 79-84.

[43] Hu H, Li H, Meng X, et al. Phase-locked schlieren of periodic nanosecond-pulsed DBD actuation in quiescent air[C]//54th AIAA Aerospace Sciences Meeting. 2016: 1696.

[44] Zhao Z, Li J M, Zheng J, et al. Study of shock and induced flow dynamics by nanosecond dielectric-barrier-discharge plasma actuators[J]. AIAA Journal, 2015, 53(5): 1336-1348.

[45] Long Y, Li H, Meng X, et al. Influence of actuating position on asymmetric vortex control with nanosecond pulse DBD plasma actuators[J]. IEEE Transactions on Plasma Science, 2016, 44(11): 2785-2795.

[46] Gao X, Yang S, Sun W. Using Global Pathway to Understand Chemical Kinetics[C]//6th International Workshop on Model Reduction in Reacting Flow. 2017.

[47] Johnson P N, Taneja T S, Yang S. Plasma-based global pathway analysis to understand the chemical kinetics of plasma-assisted combustion and fuel reforming[J]. Combustion and Flame, 2023, 255: 112927.

Highlights:

- The hydrodynamic perturbation after nSDBD excitation in a quite small time-spatial scale for $CH_4/O_2/He$ mixture with different equivalence ratio is simulated by two-dimensional plasma solver PASSKEy.
- The path flux analysis model in plasma-participant system is newly developed to reveal the kinetic effects of key plasma species and dominant global reaction paths connecting the user-defined source species to sink species.
- The energy transfer induced by gas heating during ignition of stoichiometric and lean $CH_4/O_2/He$ mixture motivated by NRP-SDBD plasma is systematically analyzed from the view of plasma kinetics.

Declaration of interests

The authors declare that they have no known competing financial interests or personal relationships that could have appeared to influence the work reported in this paper